



# The aged niche disrupts muscle stem cell quiescence

## Citation

Chakkalakal, Joe V., Kieran M. Jones, M. Albert Basson, and Andrew S. Brack. 2012. The aged niche disrupts muscle stem cell quiescence. *Nature* 490(7420): 355-360.

## Published Version

doi:10.1038/nature11438

## Permanent link

<http://nrs.harvard.edu/urn-3:HUL.InstRepos:11180414>

## Terms of Use

This article was downloaded from Harvard University's DASH repository, and is made available under the terms and conditions applicable to Other Posted Material, as set forth at <http://nrs.harvard.edu/urn-3:HUL.InstRepos:dash.current.terms-of-use#LAA>

## Share Your Story

The Harvard community has made this article openly available.  
Please share how this access benefits you. [Submit a story](#).

[Accessibility](#)

Published in final edited form as:

Nature. 2012 October 18; 490(7420): 355–360. doi:10.1038/nature11438.

## The aged niche disrupts muscle stem cell quiescence

Joe V. Chakkalakal<sup>1</sup>, Kieran M. Jones<sup>4</sup>, M. Albert Basson<sup>4</sup>, and Andrew S. Brack<sup>1,2,3</sup>

<sup>1</sup>Center of Regenerative Medicine, Massachusetts General Hospital, 185 Cambridge Street, Boston MA 2114, USA

<sup>2</sup>Harvard Stem Cell Institute, 185 Cambridge Street, Boston MA 2114, USA

<sup>3</sup>Harvard Medical School, 185 Cambridge Street, Boston MA 2114, USA

<sup>4</sup>Department of Craniofacial Development and Stem Cell Biology, King's College London, Guy's Campus, London SE1 9RT, UK

### SUMMARY

The niche is a conserved regulator of stem cell quiescence and function. During aging, stem cell function declines. To what extent and by which means age-related changes within the niche contribute to this phenomenon are unknown. We demonstrate that the aged muscle stem cell niche, the muscle fiber, expresses FGF2 under homeostatic conditions, driving a subset of satellite cells to break quiescence and lose self-renewing capacity. We show that relatively dormant aged satellite cells robustly express Sprouty1 (*spry1*), an inhibitor of FGF signalling. Increasing FGF signalling in aged satellite cells under homeostatic conditions by removing *spry1*, results in the loss of quiescence, satellite cell depletion and diminished regenerative capacity. Conversely, reducing niche-derived FGF activity through inhibition of FGFR1 signalling or overexpression of *spry1* in satellite cells prevents their depletion. These experiments identify an age-dependent change in the stem cell niche that directly influences stem cell quiescence and function.

### INTRODUCTION

Pax7-expressing satellite cells (SCs) function as an essential stem cell population capable of extensive self-renewal and skeletal muscle repair<sup>1–6</sup>. During aging, the regenerative capability of muscle is hampered due in part to impaired SC function<sup>7</sup>. Exposure to a young environment or manipulation of growth factors, which promote proliferative expansion or myogenic progression, can partially restore aged satellite cell proliferation and differentiation<sup>8–13</sup>. However, aged skeletal muscle also demonstrates a notable decline in the number of Pax7<sup>+</sup> SCs under homeostatic conditions<sup>10,13,14</sup>. The signalling cascades responsible for regenerative decline in aged muscle have been intensely investigated<sup>9,11,15</sup>, in contrast, the mechanisms driving SC depletion with age remain unknown.

In invertebrates, age-associated changes in the niche have been shown to cause a decline in stem cell number and function<sup>16,17</sup>. In mammals, the stem cell niche is a critical factor in the maintenance of quiescence, a reversible state of growth arrest crucial to the preservation of adult stem cell number and function<sup>18,19</sup>. SCs are located along the length of the muscle fibre in close contact with the plasma membrane and beneath the basal lamina<sup>20</sup>. The

### AUTHOR CONTRIBUTION

JVC designed and performed experiments, analysed data, interpreted results and wrote the manuscript. KMJ performed experiments, analysed data and edited the manuscript. MAB conceived the project, designed experiments and interpreted results, and edited the manuscript. ASB conceived the project, designed and interpreted experiments, and wrote the manuscript. The authors declare no competing financial interests.

association of adult SCs with its mature muscle fibre is of vital importance to maintain SC quiescence during homeostasis<sup>21</sup>. Therefore the muscle fiber is considered to be a component of the SC niche. Here we sought to investigate the influence of ageing on the SC niche and its impact on SC homeostasis.

## RESULTS

### Aged satellite cells cycle more frequently during homeostasis

During ageing, the number of Pax7<sup>+</sup> SCs declines (Supplementary Fig. 1a-h). Preservation of the quiescent state is a fundamental process that maintains the number and function of self-renewing stem cells<sup>22</sup>. We tested whether muscle stem cell quiescence was disrupted during aging in homeostatic conditions. Proliferative output of SCs throughout life was assessed based on label retention character (LRC). For this purpose, adult TetO-H2B-GFP mice were fed Doxycycline (Dox) for 6 weeks to transiently activate H2B-GFP and chased for 20 months to monitor proliferative output (Fig. 1a)<sup>23</sup>. During the chase period, the satellite cell pool cycled heterogeneously, with at least two distinct populations based on H2B-GFP intensity, a label retaining cell (LRC) (~35%) and a non label retaining cell (nonLRC, ~65%) populations. We next determined if the rate of satellite cell cycling differed between adult and aged H2B-GFP mice during a 12-week chase (Fig. 1b). In comparison to adult, aged SCs demonstrated a more pronounced dilution of H2B-GFP label, suggesting that aged SCs spend less time in a quiescent state. As confirmation of disrupted quiescence, we observed increased BrdU<sup>+</sup> SCs (Fig. 1c,e) and an increase in cycling (Ki67<sup>+</sup>) SCs in aged compared to adult SCs (Fig. 1d,f). Based on transcriptional analysis of sorted SCs, *myoD*, a marker of cycling SCs was higher (Fig. 1g), in contrast, quiescent markers, *p27* and *spry1*<sup>6</sup>, were lower in aged relative to adult SCs (Fig. 1h). Therefore aged SCs lose their ability to retain a quiescent state.

### Preservation of quiescence protects muscle stem cell function

We next analyzed the function of aged SCs by transplantation *in vivo* and cell fate assays *in vitro*. H2B-GFP mice were used to provide a tractable source of nuclear H2B-GFP-expressing SCs (Fig. 2a). Thirty days after transplantation into Dox-fed adult wild type hosts (Fig. 2b,c), in comparison to adult, we observed a ~60% decline in contribution from aged H2B-GFP<sup>+</sup> SCs to the myonuclear (Fig. 2d) and Pax7<sup>+</sup> compartment (Fig. 2e). Therefore, aged SCs display a cell autonomous decline in self-renewal and differentiation potential. Moreover, *in vitro* fate analysis of sorted SCs (Fig. 2f-i and Supplementary Fig. 2) demonstrates that aged SCs tend to lose markers of self-renewal potential (Pax7)<sup>24-26</sup> and gain markers of differentiation (Myogenin, MyoG)<sup>27</sup> and apoptosis (aCasp) (Fig. 2g-i). Thus, fewer SCs in aged muscle retain self-renewal potential after cell cycle entry.

We next asked whether the relative proliferative output between aged LRC and nonLRC subsets influenced SC phenotypes. Consistent with a more quiescent primitive state, aged LRCs displayed increased of *pax7*, *spry1* and *p27* and decreased *myf5* expression compared to nonLRCs (Fig. 2j). After 4 days *in vitro*, aged nonLRCs displayed reduced cell growth (Fig. 2k), loss of Pax7 (Fig. 2l), and an increase in MyoG expression compared to aged LRCs (Fig. 2m). Apoptosis was not different between aged LRC and nonLRCs (Fig. 2n). Next, aged LRC and nonLRCs were transplanted into adult, pre-injured, Dox-fed recipients and allowed to recover for 30 days (Fig. 2o). LRCs seeded approximately 3-fold more SCs and differentiated myonuclei compared to nonLRC transplant recipients (Fig. 2q,r). Together, these data demonstrate that under homeostatic conditions the SC pool is functionally heterogeneous based on proliferative history and that maintenance of quiescence is vital to retain self-renewal potential throughout life.

## FGF2 is an aged niche-derived factor that induces satellite cells into cycle

The stem cell niche is essential for quiescence and maintenance of the stem cell pool<sup>17,19</sup>. We asked whether disrupted quiescence was due to changes in the aged muscle stem cell niche, the muscle fibre<sup>21</sup>. Members of the FGF family of ligands are well-characterized growth factors that are known to possess potent satellite cell mitogenic activity<sup>28,29</sup>. We performed an array of FGF ligands, in aged and adult purified single muscle fibres. Only five FGFs were expressed in single muscle fibres and *fgf2* demonstrated the greatest fold increase in aged fibres (Fig. 3a, Supplementary Fig. 3a,b). We next used in situ hybridization to analyse *fgf2* expression (Fig. 3b). *Fgf2* was observed in restricted regions along the length of aged muscle fibers, some in close proximity to SCs (Supplementary Fig. 3c). In support, we observed a notable increase FGF2 protein underneath the basal lamina in aged relative to adult skeletal muscles, whereas FGF2 was not detected in adult and aged SCs (Fig. 3c,d and Supplementary Fig. 2d,e). Moreover, aged muscle had fewer FGF2<sup>+</sup> interstitial cells compared to adult muscle (Supplementary Fig. 2f-h). Together the results demonstrate that the aged satellite cell niche, the muscle fiber, is the principal source of FGF2.

To identify soluble muscle fiber-derived factors that signal to SCs, purified single muscle fibres were isolated, subjected to multiple washes to minimize interstitial cell contamination and soluble fractions extracted (hereafter termed purified myofiber (PM) extract) (Fig. 3e, Supplementary Fig. 4a-e). PM extract diluted in basal media was incubated with quiescent SCs (Fig. 3f,g and Supplementary Fig. 4i) and Pax7<sup>+</sup> satellite cell-like reserve cells (RSCs), a model of reversibly quiescent SCs (Supplementary Fig. 4i,k)<sup>30</sup> and assayed for cell cycle entry. In comparison to adult PM extract, aged extract increased the fraction of adult and aged quiescent cells that entered cycle (Fig. 3f and Supplementary Fig. 4i), but did not affect apoptosis (Supplementary Fig. 4f). In contrast to PM extract, aged serum did not induce cell cycle entry (Supplementary Fig. 4g)<sup>12</sup>. Moreover, aged interstitial cell extract did not induce cell proliferation (Supplementary Fig. 4d,e). Collectively, these results demonstrate that proliferative activity of SCs is induced by muscle fiber-derived factors.

To test whether FGF2 was responsible for the altered biological activity of aged PM extract, PM extract was treated with a blocking antibody to FGF2 (FGF2bl) or FGF2, prior to incubation of SCs (Fig. 3f,e and Supplementary Fig. 4h) and RSCs (Supplementary Fig. 4j,k). FGF2 added to adult PM extract was sufficient to break quiescence, and neutralization of FGF2 activity prevented aged PM extract-induced cell cycle entry (Fig. 3f and Supplementary Fig. 4h,j,k). Therefore, soluble muscle fiber-derived FGF2 is one age-related change that leads to a loss of quiescence in aged SCs.

To confirm that the active components of the PM extracts signal through FGF receptors, we pre-treated quiescent SCs and RSC cultures with the FGFR1 inhibitor, SU5402 (FGFR1i) prior to PM extract exposure. FGFR1i treatment prevented aged PM extract-induced cell proliferation (Fig. 3g, Supplementary Fig. 4l). In support, proliferation of quiescent Cre-adenovirus treated RSCs cultured from *fgfr1<sup>flx/flx</sup>* SCs was abolished in the presence of FGF2 and aged PM extract relative to control cultures (Supplementary Fig. 4m). In contrast, FGFR1i treatment and deletion of *fgfr1* did not alter proliferation of SCs or RSCs cultured with adult PM extract. Therefore, aged muscle fiber-derived FGF2 signals through FGFR1 to promote SC loss of quiescence.

To determine whether aged SC quiescence was regulated through FGF signalling *in vivo*, we asked whether long-term administration of FGFR1i would prevent SC proliferation (Fig. 3h-j). After six weeks with FGFR1i treatment, the fraction of BrdU<sup>+</sup> SCs from aged muscle was indistinguishable from adult control muscle (Fig. 3i). Moreover, the increased apoptosis observed in aged SCs was attenuated (Fig. 3j). These results demonstrate that elevated FGF

signalling is a major contributor to a loss of stem cell quiescence and possibly stem cell depletion during ageing under homeostatic conditions.

### Satellite cell quiescence in the aged niche is sensitive to acute changes in levels of FGF signalling

We next asked whether quiescent SCs were sensitive to increased levels of FGF signalling from the niche. The Sprouty (*spry*) family of genes function as downstream targets and negative feedback modulators of the FGF signalling cascade<sup>31,32</sup>. Comparison between Sprouty family members revealed that *spry1* expression unlike other Sprouty family members, was decreased by FGF2 (Supplementary Fig. 5a)<sup>33</sup> and enriched in aged LRCs compared to nonLRCs (Supplementary Fig. 5b). These data are consistent with high levels of *spry1* expression in quiescent SCs and RSCs<sup>19</sup>. To assess whether lower levels of *spry1* in nonLRCs was due to an increased number of *spry1*-negative cycling cells<sup>6</sup>, we analyzed *spry1* transcriptional activity at the single cell level using aged H2B-GFP; *Spry1*<sup>lacZ+/-</sup> mice<sup>6,34</sup>. We observed a reduction in  $\beta$ -gal staining intensity in aged quiescent (Ki67<sup>-</sup>) nonLRCs relative to LRCs and a relatively low number of cycling LRC an nonLRCs (Supplementary Fig. 5c-g). Therefore aged quiescent SCs with a limited proliferative history are enriched for the FGF inhibitor, *spry1*.

To manipulate *spry1* levels in SCs we used *Pax7CreER*<sup>TM</sup> crossed with an inducible loss-of-function (*Spry1*<sup>flx</sup>)<sup>6</sup> (*Spry1* null) and a gain-of-function (*CAG*<sup>loxP</sup>*GFP*<sup>loxP</sup>*Spry1*) (*Spry1*OX) allele<sup>35</sup> to increase and decrease FGF signalling, respectively. Tamoxifen (Tmx) was administered to *Spry1* null and control adult mice, 10 days later sorted SCs were cultured for 24 hours in FGF2, or PM extract alone, and in combination with FGF2b1 or FGFR1i. Consistent with our hypothesis, a larger fraction of *Spry1* null SCs entered the cell cycle in the presence of FGF2 (Supplementary Fig. 6a) and aged PM extract (Supplementary Fig. 6b) compared to control SCs. Moreover, the loss of quiescence induced by aged PM extract in *Spry1* null SCs was prevented in the presence of FGF2b1 and FGFR1i (Supplementary Fig. 6b,c). In contrast, aged PM extract-induced proliferation was prevented in Tmx-treated *Spry1*OX SCs compared to controls (Supplementary Fig. 6d). In support of these findings, proliferation of quiescent Cre-adenovirus treated RSCs cultured from *Spry1*<sup>flx/flx</sup> SCs was augmented in the presence of FGF2 and aged PM extract relative to control cultures (Supplementary Fig. 6e,f). In contrast, proliferation induced by FGF2 and aged PM extract was abrogated in Cre adenovirus-treated RSCs cultures from *Spry1*OX SCs (Supplementary Fig. 6g-h). Together these results demonstrate that *spry1* levels modulate FGF2-FGFR1 signalling to maintain muscle stem cell quiescence *in vitro*.

To test the requirement of *spry1* for maintaining SC quiescence *in vivo*, we administered Tmx to adult and aged control and *Spry1* null mice to delete *spry1* (Fig. 4a)<sup>6</sup>. This approach efficiently deletes *spry1* and increases a downstream transcriptional target of FGF signalling, *erm* *in vivo* (Supplementary Fig. 7). After a short-term deletion of *spry1*, the number of Pax7<sup>+</sup> cells (Fig. 4b) and percentage of cycling Pax7<sup>+</sup> cells (Fig. 4c) was significantly increased in *Spry1* null relative to control aged mice, consistent with loss of quiescence. This effect was abrogated in the presence of FGFR1i (Fig. 4b), thus providing further confirmation that Sprouty1 modulates levels of FGF signalling in aged SCs. In contrast to aged mice, deletion of *spry1* in adult mice did not alter SC number, consistent with a low level of FGF2. To further define the loss of quiescence after elevated FGF signalling under homeostasis, we assessed BrdU label retention character (BrdU-LRC), a readout of slow dividing stem cell behavior<sup>36</sup> in adult and aged *Spry1* null and control mice (Fig. 4d). Comparison of chased adult control and *Spry1* null mice revealed no shifts in BrdU-LRC of SCs. In contrast, BrdU-LRC was decreased in aged *Spry1* null relative to aged control mice. Therefore, short-term deletion of *spry1* in aged SCs leads to loss of quiescence. To ask whether Sprouty1 was sufficient to inhibit SC proliferation in aged

muscle, we analyzed aged and adult *Spry1*OX and control mice (Fig. 4e). Both *Spry1*OX and control mice received Tmx at 18 months of age, were fed BrdU at 21 months and sacrificed at 23 months of age. In comparison to aged control, fewer aged *Spry1*OX SCs incorporated BrdU, consistent with maintained SC quiescence (Fig. 4e). These results demonstrate that *spry1*, expressed specifically in SCs is sufficient to dampen FGF2-FGFR1 signalling from the aged niche to maintain cellular quiescence.

### Longer-term changes in FGF signalling levels mediate satellite cell number and function

We hypothesized that loss of quiescence driven through elevated aged niche-derived FGF2 signalling was contributing to SC depletion during ageing. To this end, we performed long-term *spry1* deletion experiments to increase FGF signalling specifically in SCs throughout adult life. *Spry1*null and control mice were administered Tmx and analysed 18 months later (Fig. 5a). Compared to aged controls, the number of SCs declined by ~50% in aged *Spry1*null muscle. We next deleted *spry1* in aged SCs, i.e. upon age-induced FGF2 increases in the niche (Fig. 5b), and analysed satellite cell number 6 weeks later. Compared to aged controls, aged *Spry1*null mice had 50% fewer SCs. When cultured, aged *Spry1*null SCs were more prone to differentiation and apoptosis compared to aged control cells (Supplementary Fig. 8). Together, these data demonstrate that aged niche-induced FGF signalling leads to an initial loss of quiescence followed by a depletion of the stem cell pool. In contrast, SC number was two-fold higher in aged *Spry1*OX compared to aged controls (Fig. 5c). Therefore levels of FGF signalling induced by the aged niche mediate SC pool size in homeostatic conditions.

The observed correlation between diminution of the SC pool (Supplementary Fig. 1)<sup>13,14</sup> and regenerative delay during aging<sup>7</sup>, prompted us to ask whether further diminution of the aged SC pool, achieved via *spry1* disruption in aged SCs impairs muscle regenerative capacity (Fig. 5d). Six weeks after Tmx delivery, aged control and *Spry1*null muscle were injured and left to recover for 30 days. In aged control mice, muscle regenerative capacity based on myofibre size was reduced by 15% compared to uninjured contralateral muscle. In aged *Spry1*null mice, the myofibre size of regenerated muscle was 50% smaller than the contralateral control (Fig. 5e). To confirm that the regenerative decline was related to SC loss, we injured aged *Spry1*null mice 10 days after Tmx administration; when the number of Pax7<sup>+</sup> cells was elevated due to initial loss of quiescence (Supplementary Fig. 9). This result demonstrates that after short-term *spry1* deletion, muscle fiber size was increased in regenerating aged *Spry1*null mice compared to aged controls (Supplementary Fig. 9). Therefore, the exacerbated loss of the SC pool due to longer-term elevated FGF signalling in aged uninjured muscle becomes limiting upon regeneration.

Finally, to test the impact of long-term inhibition of FGF signalling in response to injury, adult and aged mice were injured after six weeks FGFR1i administration (Supplementary Fig. 10). Muscle fiber size was 30% smaller in FGFR1i-treated compared to controls suggesting that repression of FGF signalling inhibits myofiber repair<sup>37,38</sup>. In contrast, the number of self renewing SCs was increased in aged FGFR1i mice compared to controls. This result demonstrates that repressing FGFR1 signalling during aging improves SC self-renewal capacity during regeneration.

## DISCUSSION

Our data demonstrate that elevated levels of FGF signalling directed from the aged SC niche leads to the loss of quiescence and depletion of the resident stem cell population, which eventually diminishes muscle regenerative capacity (Supplementary Fig. 11). That aged SCs break quiescence under homeostatic conditions was surprising considering their proliferative disadvantage in high mitogen regenerative contexts<sup>39</sup>. In support of our data, aged



hematopoietic stem cells are more active in the aged niche<sup>40,41</sup>. It is possible that a consequence of aging across stem cell niches is their inability to retain stem cells in a quiescent state.

Functional heterogeneity within the adult SC pool is becoming more apparent<sup>26,42,43</sup>. We demonstrate that the aged SC compartment is composed of highly functioning LRCs and nonLRCs that self renew poorly and tend to differentiate, demonstrating that retention of quiescence is essential for maintenance of stem cell function. Quiescence of adult SCs is regulated at multiple levels<sup>44-46</sup>. We show that SCs that retain a more quiescent phenotype and maintain stem cell function, express higher levels of the FGF inhibitor, *spry1*. Therefore, feedback inhibition of niche-derived signals may be a means to promote SC maintenance with age.

The systemic environment plays a significant role in SC proliferation *in vitro* and during repair. The young systemic environment stimulates SC proliferation; the aged systemic environment inhibits SC proliferation<sup>9,12</sup>. We now show that the aged SC niche becomes stimulatory, driving SCs out of quiescence, suggesting that the niche is dominant during homeostasis. However, in the context of injury, the relationship between niche and systemic signalling is disrupted, due to injury-induced niche (muscle fiber) degeneration. Such disruption potentially creates a permissive state for systemic environment to exert its influence on SCs.

To our knowledge, this is the first identification of a ligand that specifically increases within a mammalian aged niche that can promote breaks in quiescence leading to declines in stem cell function and number during homeostasis. The reasons behind the increased FGF2 are not known. We speculate that FGF2 induction is a cell autonomous response as an attempt to repair the aged muscle fiber, akin to the induction of FGFs during development and regeneration to promote myogenic commitment and differentiation<sup>37,38,47-50</sup>. Strategies to prevent chronic FGF2 production from the aged niche or repress FGF signaling at the level of the aged SC may reduce stem cell loss during aging.

## MATERIALS AND METHODS

### ANIMALS

C57BL/6 mice were obtained from Jackson Laboratories (Bar Harbor, ME) and the National Institute on Aging. Mice were used at 4-8 months of age (adult) or 22-24 months of age (aged). Mice carrying the *spry1* gene flanked by a pair of *loxP* sites (*Spry1<sup>flx</sup>*) were used for satellite cell specific deletion studies<sup>6,51</sup>. Mice carrying a transgene encoding a Cre inducible expression construct for *spry1* controlled by a *chicken β-actin gene (CAG)* promoter (*Spry1OX*) were used for satellite cell specific over-expression studies<sup>35</sup>. Mice carrying 1 copy of the *lacZ* gene encoding β-galactosidase inserted into the *spry1* coding region (*spry1<sup>lacZ+/-</sup>*) was used to examine *spry1* transcriptional activity<sup>34</sup>. Mice carrying the *fgfr1* gene whereby exons 8 to 14 are flanked by *loxP* sites (*FGFR1 flx*) were used in RSC deletion studies<sup>52</sup>. *Spry1<sup>flx</sup>* or *Spry1OX* mice were crossed with *Pax7-CreER<sup>TM</sup>* mice<sup>53</sup> to generate *Pax7-CreER<sup>TM</sup>; Spry1<sup>flx/flx</sup>* (*Spry1flx/flx*) or *Pax7-CreER<sup>tmx</sup>; Spry1OX/OX* (*Spry1OX/OX*) mice and control (Ctrl (-CreER)) littermates. Mice for *Cre/lox* inducible experiments were maintained on a FVB background. *TetOP-H2B-GFP* mice<sup>23</sup> and were backcrossed onto a C57BL6 background. *TetO-H2B-GFP* mice were crossed with *spry1<sup>lacZ+/-</sup>* mice to generate *TetO-H2B-GFP; spry1<sup>lacZ+/-</sup>* (*H2BGFP; Spry1lacZ+/-*) mice. Unless otherwise stated 4-6 mice were used per condition. Animals were housed and handled in accordance with the guidelines of the MGH subcommittee for animal research.

## IN-VIVO CELL DIVISION ANALYSIS

To assess cell proliferation and label retention character aged and adult C57BL/6, Ctrl, Spry1flx/flx and Spry1OX/OX mice were fed BrdU (Sigma) (0.5 mg/ml supplemented with 5% sucrose) continuously for 6 weeks. For label retention studies, Spry1flx/flx mice were given 3 daily intraperitoneal (IP) injections of Tmx (diluted in corn oil (Sigma))<sup>51</sup> following BrdU loading and placed on regular drinking water to chase label. For cell proliferation and label retention studies satellite cells (SCs) were sorted, immediately plated and processed for immunostaining with Pax7 and BrdU antibodies after sodium citrate antigen retrieval<sup>51</sup>. For label retention studies, BrdU positive SCs were classified as label retaining based on quantification of BrdU fluorescent intensity<sup>36</sup>. Fluorescence intensity of BrdU signal obtained by alexa-conjugated 546 secondary antibodies was converted to grey scale and quantified using Nikon Eclipse software. Briefly, images were taken with a 40X Plan Fluor objective using identical filter settings, gain and exposure values. Grey scale intensity and background values were obtained for each cell image. The intensities after background subtraction were then converted to logarithmic values, binned into different categories and plotted with Microsoft Excel and Graph Pad Prism software. For all conditions 300-600 cells were assessed. For transient H2B-GFP expression *in vivo*, doxycycline (Dox) (Sigma) was added to drinking water (1 mg/ml supplemented with 5% sucrose) of aged or adult H2B-GFP mice for 6 weeks. Some mice were immediately sacrificed whereas others were given normal drinking water to allow chase of H2BGFP label prior to isolation of SCs.

## IN-VIVO PHARMACOLOGICAL INHIBITION

Prolonged pharmacological inhibition of FGF activity *in vivo* was conducted as previously described (Buono et al., 2010). Initially anion exchange resin-beads (AG1×2, 200-400, CL, CAT# 1401251, BioRad) were reconstituted at a ratio of 1(beads): 2 (PBS). Half of the PBS bead mixture was pelleted at 3800rpm for 5 minutes. Pellets were then incubated with 500μM SU5402 (Calbiochem) or an equivalent volume of vehicle (DMSO) for 60 minutes on a nutator at room temperature. Loaded pellets were washed in PBS and reconstituted into 50% W/V PBS prior to IP injection of 300μl with a 25G5/8 1ml insulin syringe (BD Biosciences) into aged and adult mice. After injection, mice were fed BrdU continuously for 6 weeks prior to isolation of SCs. SCs were subsequently plated and processed for BrdU immunostaining via sodium citrate antigen retrieval<sup>51</sup>. For quantification 300-600 cells were counted per condition.

## SATELLITE CELL TRANSPLANTATION

Aged and adult H2B-GFP mice were fed Dox (1mg/ml 5% sucrose) in drinking water continuously for 6 weeks to label SCs. After Dox feeding 2000 SCs were FACS purified and reconstituted in 50μl PBS loaded with a sterile filtered pipet into 3/10ml cc, 8mm, 31G, 30 unit ultra-fine needles (BD Biosciences) for direct intramuscular delivery into host C57BL/6 tibialis anterior (TA) muscle that had been injured 1.5 day prior with 1.2% BaCl (Sigma). Host C57BL/6 mice after transplant were refed Dox (1mg/ml in 5% sucrose in drinking water) to maintain H2B-GFP label during the 30 day regeneration period after transplant. Subsequently, mice were sacrificed; transplanted TAs dissected, fixed in ice cold 4% PFA for 2 hours and incubated overnight in 30% sucrose solution. From a subset of animals, muscles were teased apart into smaller pieces, visualized in whole-mount and imaged with an inverted Nikon TS100 microscope with 4X Plan Fluor objective. For immunohistological analysis, 10μm thick transverse sections were obtained for every 200μm region. Sections were then processed with primary antibodies to Pax7 and laminin followed by incubation with goat-anti mouse 546, goat-anti chicken 647 and DAPI. Counts of H2BGFP positive myonuclei and Pax7 cells were obtained from six consecutive 10μm sections per transplant taken over three regions. Obtained numbers were then averaged and compared between



groups (see statistics). Three transplants were performed for each condition. All images were taken and processed with Nikon Eclipse and Adobe Photoshop CS software.

### PURIFIED MUSCLE FIBRE (PM) EXTRACT

Initially fore and hind-limb muscles were cut into smaller longitudinal pieces and digested into single or smaller groups of muscle fibers (0.2% collagenase, DMEM) in a horizontal shaking water bath at 37°C for 90 minutes<sup>6</sup>. Isolated single muscle fibers were gently triturated and repeatedly washed in PBS (6×) to ensure removal of interstitial cells or other contaminating debris. Purified single fibers were then incubated in a high salt extraction buffer (400mM NaCl, 1mM EGTA, 1mM EDTA, 10mM Tris pH 7.5, 1mg/ml PMSF) to dissociate any ligands bound to receptors or the extensive basal lamina network of skeletal muscle fibers<sup>54</sup>. Dissected muscles in extraction buffer were further triturated with a glass Pasteur pipette to dissociate bound ligands. The muscle fiber mixture was centrifuged at 3850rpm for 10 mins to remove cytoskeletal and nuclear elements that compromise the majority of skeletal muscle fiber cytosol. The resultant supernatant was collected and spun at 1500rpm for 5 mins. Supernatant was then collected and transferred into eppendorf tubes and spun at 16500g for 30mins at 4°C. The supernatant was pooled and subsequently drawn up into a 20-gauge syringe and filtered through a 0.45µm filter into Amicon Ultra centrifugal filter columns (10 000 MWCO, UFC901008, Millipore). Exchanges with PBS were done at 3500rpm for 20 mins until the solution was translucent and concentrated into a volume of approximately 1ml PBS. Protein concentration and purity was determined with a nanodrop analyzer. To assess cycling inducing activity cultures of RSCs and SCs in basal media (3% HS for RSCs and 5% HS for SCs in DMEM) were incubated with 10µg total of PM extract for a 24 hour period. For inhibition of FGF activity RSCs and SCs were incubated with 10µM SU5402 or DMSO prior to incubation with PM extracts. For FGF2 neutralization niche extracts were incubated with 15ng/µl FGF2 blocking antibody (FGF2bl) (Millipore) for 1 hour prior to adding to RSC or SC cultures. Unless otherwise stated 3-5 experiments were performed in triplicate and 300-600 RSCs or SCs were counted. PM extracts were obtained from n=5 different aged and adult mice and examined.

### SINGLE MUSCLE FIBRE AND MYOGENIC CELL PREPARATION

Single muscle fibres and satellite cell isolations were performed as described elsewhere<sup>24</sup> To generate RSC cultures<sup>6,30</sup>, low-passage primary myoblasts were plated in 1/500 ECM coated 8-well permanox chamber slides (LabTek) at 80-90% confluency and maintained in growth media (20% FBS, 5 ng/ml bFGF in Ham's F-10). Subsequently, cells were switched to differentiation media (3% HS in DMEM) for 2 days to allow the formation of myotubes and satellite cell-like RSCs expressing Pax7 that have escaped differentiation and returned to a quiescent state<sup>30</sup>. RSC cultures were then treated with appropriate PM extracts (described above) 24 hours. For adenovirus experiments (see below) cells were infected after formation of myotubes and RSCs and allowed to recover for 24 hours prior to treatment with extracts.

### ACTIVATION OF CRE RECOMBINASE

Cultures of RSCs were infected with either Ad5CMVCre-eGFP or Ad5CMV-eGFP-control adenovirus (Gene Transfer Vector Core, University of Iowa) for 1.5 hr at 37°C. Cells were washed in PBS and incubated in fresh differentiation media for an additional 48 hr. Aged and adult mice were given IP injections of Tmx<sup>6</sup>

### FLUORESCENT-ACTIVATED CELL SORTING

To obtain highly purified myogenic cells, mononucleated cells were isolated from uninjured and regenerating muscle as described<sup>6</sup> with modifications. Cells were incubated in Sorting

media (10% HS, in Hams F10) for 10 min then incubated in biotin conjugated anti-VCAM1 (Novus) and anti-mouse-integrin-  $\alpha$  7 (MBL) for 30 min. Cells were washed in sorting media and spun at 1500 rpm for 5 min. Cells were stained in CD31-PE (BD Biosciences), CD45-PE (BD Biosciences), Pacific Blue (Invitrogen), and strepavidin-647 (Invitrogen) for 30 min. Myogenic cells had the following profile: VCAM1<sup>+</sup>, integrin- $\alpha$ 7<sup>+</sup>, CD31<sup>-</sup>, CD45<sup>-</sup>, PI<sup>-</sup>. Cells were sorted with FACS Aria (BD Biosciences).

## HISTOLOGY AND IMMUNOFLOURESCENCE

Cultures of RSCs and SCs and tibialis anterior (TA) tissue sections were fixed in 4% PFA for 5 min, washed and processed for immunohistochemistry as previously described<sup>6</sup>. For detection of FGF2 in transverse orientation sections were not fixed. For longitudinal sections samples were processed for primary FGF2 antibody prior to fixation. For BrdU detection, cultures of SCs, RSCs and tissue sections were fixed in 4% PFA, washed in PBS, and then antigen-retrieved with sodium citrate buffer (10 mM, 0.05% Tween in PBS) at 95°C for 30 min prior to immunostaining as previously described<sup>51</sup>.

## REAGENTS AND ANTIBODIES

The source and concentration of antibodies: Rat anti-BrdU (1/500, Abcam), rabbit anti-ki67 (1/500, Abcam) mouse anti-Pax7 (1/100, DSHB), rabbit anti-Myogenin (1/250, Santa Cruz), Cleaved Caspase-3 (1/500, Cell Signaling Technologies), chick anti-Laminin (1/5000, Abcam), VCAM (1/100), mouse anti-Integrin- $\alpha$ 7 (1/200, MBL), CD31-PE, CD45-PE (1/200, BD) and rabbit anti-FGF2 (1/500 Abcam). The corresponding species-specific Alexa conjugated (Pacific Blue, 488, 546, 647) secondary antibodies (Molecular probes) were used at 1/1500 for immunohistochemistry or 1/200 for FACS. Tamoxifen was from Sigma (St. Louis, MO). SU5402 was used as an FGFR inhibitor for in vitro (10  $\mu$ M diluted in DMSO) and in vivo studies (Calbiochem). Basic FGF2 was from R&D Systems (Minneapolis, MN). Blocking antibody to FGF2 (FGF2bl) was from Millipore.

## MUSCLE INJURY

Injury to whole TA/EDL muscle was made by injection of barium chloride (BaCl<sub>2</sub>) (50 ml, 1.2%) into 30 sites in the lower limb. This produced an extensive injury resulting in homogenous damage and activation of satellite cells<sup>6</sup>. After regeneration, the size of regenerating muscle fibers (denoted by central nucleation) and non-regenerating fibers from uninjured muscle were quantified. Briefly, muscle cross-sections were quantified through a 10X objective at three regions in the mid-belly of each muscle. Images were collected and average muscle fiber size was determined using Nikon Elements software as described previously<sup>6</sup>.

## ANALYSIS OF SATELLITE CELLS AND THEIR PROGENY

Muscles sections were stained with a cocktail of antibodies to determine the number of Pax7<sup>+</sup> satellite cells that were quiescent (Pax7<sup>+</sup>, Ki67<sup>-</sup>) or cycling (Pax7<sup>+</sup>, Ki67<sup>+</sup>) underneath the basal lamina (laminin<sup>+</sup>). The total number of Pax7<sup>+</sup> cells was quantified in a minimum of 10 serial sections per muscle in 3 separate regions from the mid-belly of the muscle<sup>6</sup>. The number of Pax7 cells was quantified on freshly isolated single EDL muscle fibers. A minimum of 20-30 muscle fibers were counted per animal<sup>6</sup>. Cultures of RSCs and SCs in 8-well permanox chamber slides (Nunc) were stained with a panel of antibodies to characterize myogenic cells with renewal potential (Pax7<sup>+</sup>), cycling (Pax7<sup>+</sup>, Ki67<sup>+</sup>) apoptosis (activated Caspase-3<sup>+</sup>) and differentiation (Myogenin<sup>+</sup>)<sup>6</sup>. For fate analysis, quantification of 3-5 experiments was performed in triplicate and 300-600 cells were counted per condition. To assess cell growth, SCs were plated at clonal density (10-12 cells/well, Nunc 8-well permanox chamber slides) and the number of cells present in each

individual well was determined after 4 days in culture (10% HS, DMEM). For cell growth experiments, 21-28 clonal density cultures were examined per condition. Wells with no cells present after 4 days of culture were not included in quantification. For LRCs 19/21 and nonLRCs 21/28 wells had cells present after 4 days of culture.

## RNA ISOLATION AND RT-PCR

RNA extraction from approximately 10,000 FACS-sorted SCs and 50 single muscle fibers was done with Trizol (Invitrogen) according to manufacturers suggested modifications by the addition of ultrapure glycogen (Invitrogen) and prepared for qRT-PCR analysis or array analysis. First-strand cDNA was synthesized from 4 $\mu$ l of RNA by the SuperScript First-Strand cDNA Synthesis Kit (Invitrogen). Quantitative real-time PCR was performed on the a Step One Plus Real time PCR machine (Applied Biosystems), with Platinum SYBR Green qPCR SuperMix-UDG with ROX master mix (Invitrogen) using primers *against pax7, myf5, myoD, spry1, spry2, spry4, p27, fgf1, fgf2, fgf6, fgfr1, fgfr4 and gapdh* (all primers are available upon request). All reactions for Real time qPCR were performed using the following thermal cyclers conditions: 50°C for 2 min, 95°C for 2 min followed by 40 cycles of a 2 step reaction; denaturation at 95°C for 15 sec, annealing at 60°C for 30 sec. Analysis of FGF ligands was conducted with the mouse growth factor RT<sup>2</sup>Profiler™ PCR array system (SABiosciences) according to manufacturers' recommendations with the exception that RNA was extracted via Trizol method. Unless otherwise stated data were from 3 separate reactions performed in triplicate from n=4-6 mice each condition.

## WHOLE MOUNT IN SITU HYBRIDIZATION

Single muscle fibers were isolated and processed for *in situ* hybridization. Purified single muscle fibres were fixed in 4% PFA, washed in methanol and rehydrated in a methanol/PBST (PBS, 0.5% tween) series. Muscle fibers were then digested in 20ng/ml proteinase K (sigma) in PBST, rinsed and incubated in 4%PFA. For pre-hybridization, muscle fibers were rinsed in PBST then incubated with hybridization mix (50% formamide, 5% SSC, 0.5% tween) for 4hrs at 70°C. After prehybridization muscle fibers were incubated with sense or anti-sense probes for *fgf2* in hybridization solution overnight at 70°C. Probe was removed with a formamide/SSCT series. Single muscle fibres were washed in blocking solution (10% BSA, 2% FCS and MABT (Roche)). For probe detection, muscle fibres were incubated with anti-DIG (Roche) 1/10000 in blocking solution overnight at 4°C. The following day muscle fibers were washed with blocking solution and processed for DIG detection fixed and mounted. In some cases, after fixation and prior to mounting muscle fibres were further processed for Pax7 immunostaining as described elsewhere<sup>6</sup>.

## STATISTICS

Unless otherwise stated all are data represented as mean  $\pm$  s.e.m.; \*P<0.05 t-test. For multiple comparisons ANOVA with Bonferroni's multiple comparison post hoc test were used.

## Supplementary Material

Refer to Web version on PubMed Central for supplementary material.

## Acknowledgments

We thank Hanno Hock and Konrad Hochedlinger (Massachusetts General Hospital), and Robert Friesel (Maine Medical Research Institute) for the generous provision of reagents. Gabi Estrada for technical assistance. We are also grateful to Laura Prickett-Rice, Kat Folz-Donahue and Meredith Weglarz of the FACS core facility. This work was supported by MGH startup funds, Harvard Stem Cell Institute grants and NIH grants (R01 AR060868, R01

AR061002) to ASB, Wellcome Trust (WT091475) to MAB, JVC a MGH ECOR Postdoctoral Fellow Award and BBSRC Doctoral Training Award to KMJ.

## BIBLIOGRAPHY

1. Sambasivan R, et al. Pax7-expressing satellite cells are indispensable for adult skeletal muscle regeneration. *Development*. 2011; 138:3647–3656. doi:10.1242/dev.067587. [PubMed: 21828093]
2. Collins CA, et al. Stem cell function, self-renewal, and behavioral heterogeneity of cells from the adult muscle satellite cell niche. *Cell*. 2005; 122:289–301. [PubMed: 16051152]
3. Lepper C, Partridge TA, Fan CM. An absolute requirement for Pax7-positive satellite cells in acute injury-induced skeletal muscle regeneration. *Development*. 2011; 138:3639–3646. doi:10.1242/dev.067595. [PubMed: 21828092]
4. Sacco A, Doyonnas R, Kraft P, Vitorovic S, Blau HM. Self-renewal and expansion of single transplanted muscle stem cells. *Nature*. 2008; 456:502–506. [PubMed: 18806774]
5. Murphy MM, Lawson JA, Mathew SJ, Hutcheson DA, Kardon G. Satellite cells, connective tissue fibroblasts and their interactions are crucial for muscle regeneration. *Development*. 2011; 138:3625–3637. doi:10.1242/dev.064162. [PubMed: 21828091]
6. Shea KL, et al. Sprouty1 regulates reversible quiescence of a self-renewing adult muscle stem cell pool during regeneration. *Cell Stem Cell*. 2010; 6:117–129. [PubMed: 20144785]
7. Shavlakadze T, McGeachie J, Grounds MD. Delayed but excellent myogenic stem cell response of regenerating geriatric skeletal muscles in mice. *Biogerontology*. 2010; 11:363–376. doi:10.1007/s10522-009-9260-0. [PubMed: 20033288]
8. Carlson BM, Faulkner JA. Muscle transplantation between young and old rats: age of host determines recovery. *Am.J.Physiol.* 1989; 256:C1262–C1266. [PubMed: 2735398]
9. Brack AS, et al. Increased Wnt signaling during aging alters muscle stem cell fate and increases fibrosis. *Science*. 2007; 317:807–810. [PubMed: 17690295]
10. Collins CA, Zammit PS, Ruiz AP, Morgan JE, Partridge TA. A population of myogenic stem cells that survives skeletal muscle aging. *Stem Cells*. 2007; 25:885–894. [PubMed: 17218401]
11. Conboy IM, Conboy MJ, Smythe GM, Rando TA. Notch-mediated restoration of regenerative potential to aged muscle. *Science*. 2003; 302:1575–1577. [PubMed: 14645852]
12. Conboy IM, et al. Rejuvenation of aged progenitor cells by exposure to a young systemic environment. *Nature*. 2005; 433:760–764. [PubMed: 15716955]
13. Shefer G, Van de Mark DP, Richardson JB, Yablonka-Reuveni Z. Satellite-cell pool size does matter: defining the myogenic potency of aging skeletal muscle. *Dev.Biol.* 2006; 294:50–66. [PubMed: 16554047]
14. Brack AS, Bildsoe H, Hughes SM. Evidence that satellite cell decrement contributes to preferential decline in nuclear number from large fibres during murine age-related muscle atrophy. *J.Cell Sci.* 2005; 118:4813–4821. [PubMed: 16219688]
15. Carlson ME, Hsu M, Conboy IM. Imbalance between pSmad3 and Notch induces CDK inhibitors in old muscle stem cells. *Nature*. 2008; 454:528–532. [PubMed: 18552838]
16. Pan L, et al. Stem cell aging is controlled both intrinsically and extrinsically in the *Drosophila* ovary. *Cell Stem Cell*. 2007; 1:458–469. doi:10.1016/j.stem.2007.09.010. [PubMed: 18371381]
17. Boyle M, Wong C, Rocha M, Jones DL. Decline in self-renewal factors contributes to aging of the stem cell niche in the *Drosophila* testis. *Cell Stem Cell*. 2007; 1:470–478. doi:10.1016/j.stem.2007.08.002. [PubMed: 18371382]
18. Voog J, Jones DL. Stem cells and the niche: a dynamic duo. *Cell Stem Cell*. 2010; 6:103–115. doi:10.1016/j.stem.2010.01.011. [PubMed: 20144784]
19. Morrison SJ, Spradling AC. Stem cells and niches: mechanisms that promote stem cell maintenance throughout life. *Cell*. 2008; 132:598–611. doi:10.1016/j.cell.2008.01.038. [PubMed: 18295578]
20. Mauro A. Satellite cell of skeletal muscle fibers. *The Journal of biophysical and biochemical cytology*. 1961; 9:493–495. [PubMed: 13768451]
21. Bischoff R. Interaction between satellite cells and skeletal muscle fibers. *Development*. 1990; 109:943–952. [PubMed: 2226207]

22. Orford KW, Scadden DT. Deconstructing stem cell self-renewal: genetic insights into cell-cycle regulation. *Nat.Rev.Genet.* 2008; 9:115–128. [PubMed: 18202695]
23. Foudi A, et al. Analysis of histone 2B-GFP retention reveals slowly cycling hematopoietic stem cells. *Nat.Biotechnol.* 2009; 27:84–90. [PubMed: 19060879]
24. Zammit PS, et al. Muscle satellite cells adopt divergent fates: a mechanism for self-renewal? *J.Cell Biol.* 2004; 166:347–357. [PubMed: 15277541]
25. Olguin HC, Olwin BB. Pax-7 up-regulation inhibits myogenesis and cell cycle progression in satellite cells: a potential mechanism for self-renewal. *Dev.Biol.* 2004; 275:375–388. [PubMed: 15501225]
26. Rocheteau P, Gayraud-Morel B, Siegl-Cachedenier I, Blasco MA, Tajbakhsh SA. subpopulation of adult skeletal muscle stem cells retains all template DNA strands after cell division. *Cell.* 2012; 148:112–125. doi:10.1016/j.cell.2011.11.049. [PubMed: 22265406]
27. Yablonka-Reuveni Z, Rivera AJ. Temporal expression of regulatory and structural muscle proteins during myogenesis of satellite cells on isolated adult rat fibers. *Dev.Biol.* 1994; 164:588–603. [PubMed: 7913900]
28. Sheehan SM, Allen RE. Skeletal muscle satellite cell proliferation in response to members of the fibroblast growth factor family and hepatocyte growth factor. *J.Cell Physiol.* 1999; 181:499–506. [PubMed: 10528236]
29. Bischoff R. A satellite cell mitogen from crushed adult muscle. *Dev.Biol.* 1986; 115:140–147. [PubMed: 3699242]
30. Yoshida N, Yoshida S, Koishi K, Masuda K, Nabeshima Y. Cell heterogeneity upon myogenic differentiation: down-regulation of MyoD and Myf-5 generates ‘reserve cells’. *J.Cell Sci.* 1998; 111(Pt 6):769–779. [PubMed: 9472005]
31. Hacohen N, Kramer S, Sutherland D, Hiromi Y, Krasnow MA. sprouty encodes a novel antagonist of FGF signaling that patterns apical branching of the Drosophila airways. *Cell.* 1998; 92:253–263. [PubMed: 9458049]
32. Kim HJ, Bar-Sagi D. Modulation of signalling by Sprouty: a developing story. *Nat.Rev.Mol.Cell Biol.* 2004; 5:441–450. [PubMed: 15173823]
33. Gross I, Bassit B, Benezra M, Licht JD. Mammalian sprouty proteins inhibit cell growth and differentiation by preventing ras activation. *J.Biol.Chem.* 2001; 276:46460–46468. [PubMed: 11585837]
34. Thum T, et al. MicroRNA-21 contributes to myocardial disease by stimulating MAP kinase signalling in fibroblasts. *Nature.* 2008; 456:980–984. [PubMed: 19043405]
35. Yang X, et al. Overexpression of Spry1 in chondrocytes causes attenuated FGFR ubiquitination and sustained ERK activation resulting in chondrodysplasia. *Dev.Biol.* 2008; 321:64–76. [PubMed: 18582454]
36. Wilson A, et al. Hematopoietic stem cells reversibly switch from dormancy to self-renewal during homeostasis and repair. *Cell.* 2008; 135:1118–1129. [PubMed: 19062086]
37. Floss T, Arnold HH, Braun T. A role for FGF-6 in skeletal muscle regeneration. *Genes Dev.* 1997; 11:2040–2051. [PubMed: 9284044]
38. Lefaucheur JP, Sebille A. Muscle regeneration following injury can be modified in vivo by immune neutralization of basic fibroblast growth factor, transforming growth factor beta 1 or insulin-like growth factor I. *Journal of neuroimmunology.* 1995; 57:85–91. [PubMed: 7706442]
39. Conboy IM, Rando TA. The regulation of Notch signaling controls satellite cell activation and cell fate determination in postnatal myogenesis. *Dev.Cell.* 2002; 3:397–409. [PubMed: 12361602]
40. Morrison SJ, Wandycz AM, Akashi K, Globerson A, Weissman IL. The aging of hematopoietic stem cells. *Nature medicine.* 1996; 2:1011–1016.
41. Sudo K, Ema H, Morita Y, Nakauchi H. Age-associated characteristics of murine hematopoietic stem cells. *The Journal of experimental medicine.* 2000; 192:1273–1280. [PubMed: 11067876]
42. Ono Y, et al. Slow-dividing satellite cells retain long-term self-renewal ability in adult muscle. *Journal of cell science.* 2012 doi:10.1242/jcs.096198.
43. Kuang S, Kuroda K, Le Grand F, Rudnicki MA. Asymmetric self-renewal and commitment of satellite stem cells in muscle. *Cell.* 2007; 129:999–1010. doi:10.1016/j.cell.2007.03.044. [PubMed: 17540178]



44. Bjornson CR, et al. Notch Signaling is Necessary to Maintain Quiescence in Adult Muscle Stem Cells. *Stem Cells*. 2011 doi:10.1002/stem.773.
45. Cheung TH, et al. Maintenance of muscle stem-cell quiescence by microRNA-489. *Nature*. 2012; 482:524–528. doi:10.1038/nature10834. [PubMed: 22358842]
46. Mourikis P, et al. A Critical Requirement for Notch Signaling in Maintenance of the Quiescent Skeletal Muscle Stem Cell State. *Stem Cells*. 2011 doi:10.1002/stem.775.
47. Lagha M, et al. Pax3 regulation of FGF signaling affects the progression of embryonic progenitor cells into the myogenic program. *Genes Dev*. 2008; 22:1828–1837. [PubMed: 18593883]
48. Groves JA, Hammond CL, Hughes SM. Fgf8 drives myogenic progression of a novel lateral fast muscle fibre population in zebrafish. *Development*. 2005; 132:4211–4222. [PubMed: 16120642]
49. Flanagan-Steet H, Hannon K, McAvoy MJ, Hullinger R, Olwin BB. Loss of FGF receptor 1 signaling reduces skeletal muscle mass and disrupts myofiber organization in the developing limb. *Dev.Biol*. 2000; 218:21–37. [PubMed: 10644408]
50. Kudla AJ, et al. The FGF receptor-1 tyrosine kinase domain regulates myogenesis but is not sufficient to stimulate proliferation. *J.Cell Biol*. 1998; 142:241–250. [PubMed: 9660877]

## SUPPLEMENTARY BIBLIOGRAPHY

51. Basson MA, et al. Sprouty1 is a critical regulator of GDNF/RET-mediated kidney induction. *Dev.Cell*. 2005; 8:229–239. [PubMed: 15691764]
52. Xu X, Qiao W, Li C, Deng CX. Generation of Fgfr1 conditional knockout mice. *Genesis (New York, N.Y. : 2000)*. 2002; 32:85–86.
53. Nishijo K, et al. Biomarker system for studying muscle, stem cells, and cancer in vivo. *FASEB J*. 2009
54. Umemori H, Linhoff MW, Ornitz DM, Sanes JR. FGF22 and its close relatives are presynaptic organizing molecules in the mammalian brain. *Cell*. 118(2004):257–270. doi:10.1016/j.cell.2004.06.025. [PubMed: 15260994]

### METHODS SUMMARY

To monitor proliferative history of SCs, adult and aged *TetOP-H2B-GFP* mice received doxycycline (Dox) (1 mg/ml supplemented with 5% sucrose in drinking water) for 6 weeks<sup>23</sup>. Alternatively, mice were fed BrdU (Sigma) (0.5 mg/ml supplemented with 5% sucrose) in drinking water. Some mice were immediately sacrificed whereas others were given normal drinking water to allow chase of BrdU or H2B-GFP label prior to isolation of SCs. For SC transplantation studies, after 6 weeks Dox feeding, 2,000 SCs were FACS purified and reconstituted in 50  $\mu$ l PBS for direct intramuscular delivery into pre-injured (with 1.2% BaCl<sub>2</sub>) host C57BL/6 tibialis anterior (TA) muscle. Host mice were refed Dox (1mg/ml in 5% sucrose in drinking water) to maintain H2B-GFP label during the 30 day regeneration period. Subsequently, muscle was prepared for analysis. For immunohistological analysis, 10  $\mu$ m thick transverse sections were obtained for every 200  $\mu$ m region to identify H2B-GFP<sup>+</sup> regions. Counts of H2B-GFP<sup>+</sup> myonuclei and Pax7 cells were obtained and summed from six consecutive 10  $\mu$ m sections per transplant taken over three regions.

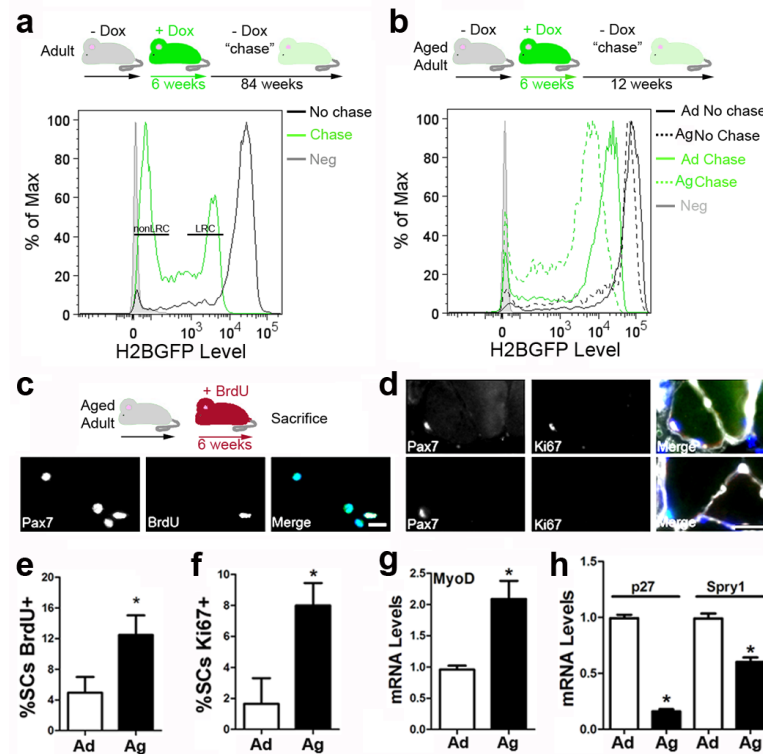


**Figure 1. Aged satellite cells cycle more frequently during homeostasis**

**a**, Doxycycline (Dox) loading and chase strategy of *TetO-H2B-GFP* mice and FACS plots for No chase and 84-week chase. SC pool has LRC and nonLRC subsets. **b**, Strategy and FACS plots for aged (Ag) or adult (Ad) no chase and 12-week chase SCs. Vehicle treated SCs (Neg) (n=10,000 cells, 6 animals/group). **c**, BrdU feeding and representative images of SCs stained with anti-Pax7, BrdU and Dapi. **d**, Representative sections from aged muscle stained with anti-Pax7, Ki67 and laminin. **e**, Percentage of BrdU<sup>+</sup> SCs (n=300 cells, 4-6 animals/group). **f**, Percentage of Ki67<sup>+</sup>/Pax7<sup>+</sup> SCs/section (n=4-6 animals/group). **g**, **h**, RTqPCR; *myod* (**g**) *p27* and *spry1* (**h**) in SCs. (n=10,000 cells/condition performed in triplicate, 5 mice/group). Scale-bar; 20  $\mu$ m, \*P<0.05, s.e.m.

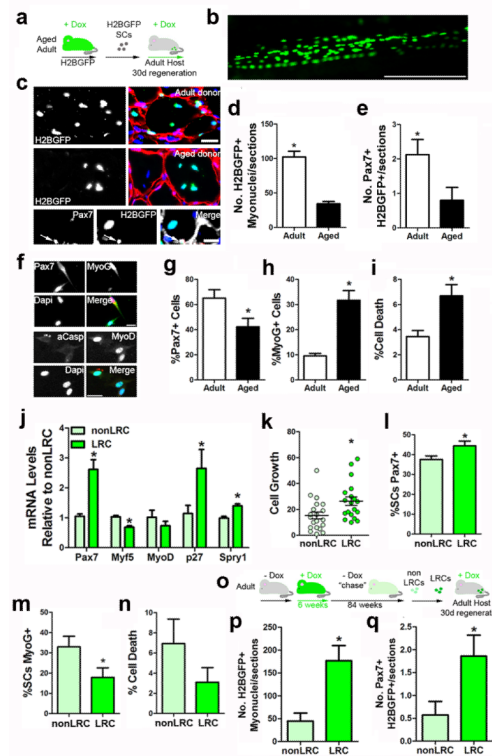


**Figure 2. Preservation of quiescence protects satellite cell function**

**a**, Scheme of transplantation assay of 2,000 aged and adult Dox-fed *TetO-H2B-GFP* SCs into pre-injured Dox-fed wildtype hosts. Representative images of host whole-mount (**b**) and muscle sections of transplant recipients (**c**) lower panels: Pax7<sup>+</sup>/H2B-GFP<sup>+</sup> cell, (Scale-bar 10μm). **d**, **e**, Number of H2B-GFP<sup>+</sup>/myonuclei (**d**) and Sublamina H2B-GFP<sup>+</sup>/SCs (**e**) summed over six consecutive 10μm sections, averaged across three regions of muscle (n=4 mice/group). **f**, Representative image of Pax7<sup>+</sup>, MyoG<sup>+</sup>, MyoD<sup>+</sup>, and activated-caspase-3<sup>+</sup> (aCasp) SCs after 4-day culture (4d). **g-i**, Percentage of Pax7<sup>+</sup> (**g**) MyoG<sup>+</sup> (**h**) and aCasp<sup>+</sup> SCs (**i**) after 4d (n=300-600 cells, in triplicate). **j**, Myogenic and quiescent marker expression (n=3 mice/condition). **k-n**, Number cells/clone (**k**) Percent Pax7<sup>+</sup> (**l**), MyoG<sup>+</sup> (**m**) and aCasp<sup>+</sup> (**n**) after 4d (n=300-5=600 cells, in triplicate). **o**, Transplant strategy of 2,000 LRC and nonLRCs injected into pre-injured Dox-fed wildtype hosts. **q**, **p**, Number of H2B-GFP<sup>+</sup>/myonuclei (**p**) Sublamina-H2B-GFP<sup>+</sup>/SCs (**q**) summed over six consecutive 10μm section, averaged across three regions of muscle (n=4 mice/group). Scale-bar; (**b**, **f**) 25μm **c**) 200μm. \*P<0.05, s.e.m.

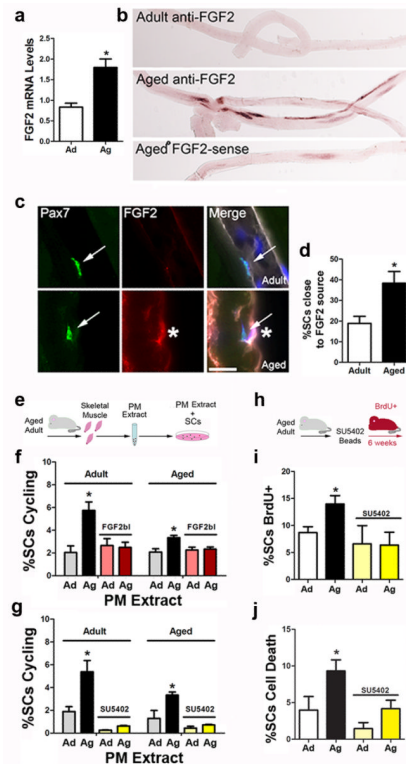


**Figure 3. FGF2 is an aged niche factor that induces satellite cells into cycle**

**a**, Single muscle fibre expression of *fgf2* by RT-qPCR (3 reactions performed in triplicate,  $n=5$  mice/group). **b**, *Fgf2* *in-situ* hybridizations on adult and aged single muscle fibers. Sense probe was used as a background negative control (lower panel). **c**, Representative longitudinal sections stained with anti-Pax7 (green, white arrow) laminin (white) and FGF2 (red) Dapi (blue) shows Pax7<sup>+</sup> SC (white arrow) close to FGF2 (asterisk). **d**, Percentage of SCs near FGF2<sup>+</sup> regions (<20 $\mu$ m) ( $n=3$  animals/group). **e**, Strategy to assess mitogenic activity of purified muscle fibre (PM) extracts. **f**, **g**, Percentage of cycling (Ki67<sup>+</sup>) adult and aged SCs treated with adult (Ad) or aged (Ag) PM extract and FGF2-blocking antibody (FGF2bl) (**f**) or SU5402 (**g**) ( $n=1000$  cells/condition,  $n=5$  animals/group). **h**, Strategy to inhibit FGF-activity *in-vivo* via implanted SU5402 coated beads. **i**, **j**, Percent BrdU<sup>+</sup>/SCs (**i**) and aCasp<sup>+</sup>/SCs 4d (**j**) after 4d from Ad and Ag mice with SU5402 treatment ( $n=300-600$  cells/condition, 4-6 mice/group). Scale=20 $\mu$ m. \* $P<0.05$ ,  $\pm$  s.e.m.



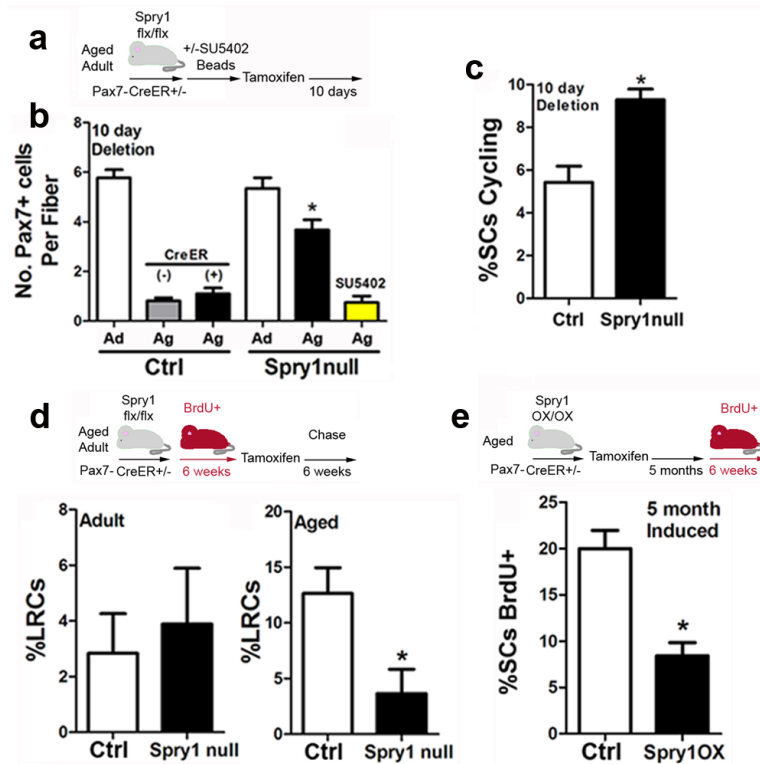


**Figure 4. Aged satellite cells are sensitive to acute changes of FGF signalling**

**a-c**, Strategy to delete Spry1 in SCs of adult (Ad) and aged (Ag) mice prior to injection of SU5402-coated beads (**b**) number of Pax7<sup>+</sup> SCs/single muscle fibre (20-30 single muscle fibers/animal, n=4-6 mice/group) (**c**) percent Ki67<sup>+</sup>/Pax7<sup>+</sup> SCs per 10 $\mu$ m cross-section 10 days post Tmx (n= 4-6 animals/group). **d**, Strategy to label and chase BrdU in SCs from Ad and Ag Ctrl or Spry1null mice 6 weeks post Tmx injection and Percent BrdU<sup>+</sup>/LRC SCs after chase. **e**, Strategy for BrdU incorporation in Tmx-treated Ctrl and Spry1OX aged mice and Percent BrdU<sup>+</sup>/SCs after chase. For panels d and e, n=1000 cells /condition, 4-6 mice/group. \*P<0.05  $\pm$  s.e.m.

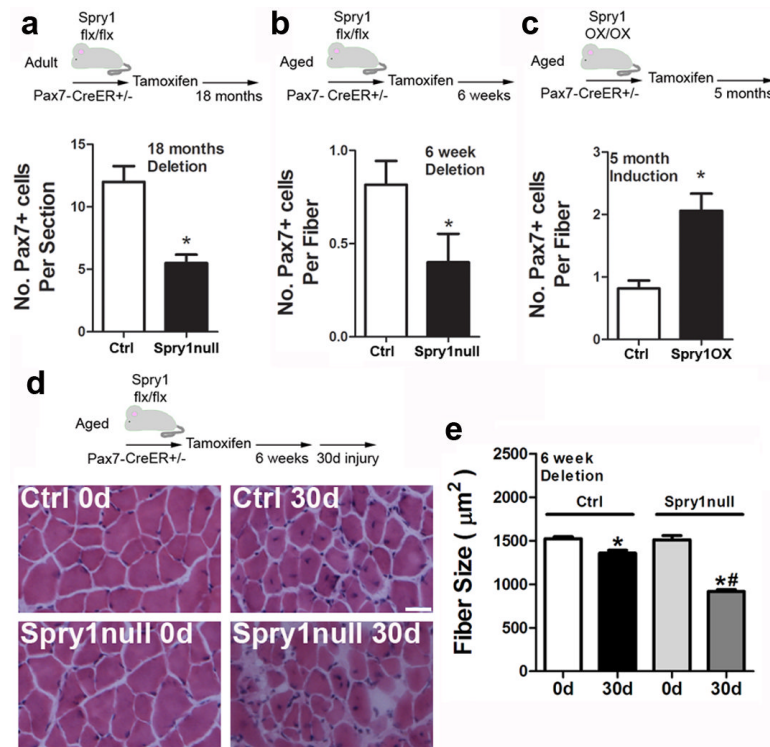


**Figure 5. Longer-term changes in FGF signalling drive satellite cell depletion**

**a**, Strategy to delete *Spry1* from SCs for 18 months and number of Pax7<sup>+</sup> SCs /muscle section (n=30 sections/muscle, 5-6 animals/group). **b**, *Spry1* deletion in aged SCs for 6 weeks and number of Pax7<sup>+</sup> SCs/single muscle fibre (n=30 fibers/animal, 5-6 animals/group). **c**, *Spry1* over-expression for 5 months in aged SCs and number of Pax7<sup>+</sup> SCs/single muscle fibre from aged Ctrl and *Spry1*OX mice (20-30 single fibers/animal, 4-6 mice/group). **d**, Prior deletion of *Spry1* for 6 weeks in aged SCs followed by muscle injury and H&E images of uninjured (0d) and 30 day (30d) regenerated muscles. **e**, Quantification of fibre size 30 days after BaCl<sub>2</sub>-induced injury (30d) and contra-lateral uninjured (0d) (scale-bar =25μm) (n=30 sections/muscle, 4-6 mice/group). \*P<0.05 to 0d, #P<0.05 to Ctrl-30d, ± s.e.m. ANOVA with Bonferroni's post-hoc test.